SCIENTIFIC REP♦RTS

OPEN

A comparative Raman study between $PrMnO_3$, $NdMnO_3$, $TbMnO_3$ and $DyMnO_3$

Sabeur Mansouri[1], Serge Jandl[1], Alexander Mukhin[2], Vsevolod Yu Ivanov[2] & Anatoly Balbashov[3]

In this paper, we present a detailed Raman study of the non-multiferroic compounds $PrMnO_3$ and $NdMnO_3$ and the multiferroic compounds $TbMnO_3$ and $DyMnO_3$ as a function of temperature and magnetic field. All studied systems show anomalous phonon shifts close to the Néel transition T_N. In $PrMnO_3$ and $NdMnO_3$, the frequency softenings are partly attributed to an orbital-spin-phonon coupling whereas in $TbMnO_3$ and $DyMnO_3$, the relatively weak frequency shifts are rather attributed to an expansion of the $Mn-O$ bond lengths. On the other hand, the frequencies of $TbMnO_3$ phonons are shifted as a function of magnetic field, while those of $PrMnO_3$ remain unaffected. These frequency shifts are interpreted in terms of local oxygen rearrangements under magnetic field that could play an important role in the multiferroicity of $TbMnO_3$ and $DyMnO_3$.

In the last decade, the study of the perovskite manganites $RMnO_3$ (R = lanthanides, Y and Bi) have attracted a considerable interest because of their fascinating properties such as colossal magnetoelectric and magnetocaloric effects[1,2]. Their physical properties are determined by a delicate interplay of charge, spin, orbital, and lattice degrees of freedom[3–5]. The study of the coupling between the lattice and the magnetic properties of these compounds represents an interesting starting point to understand the microscopic parameters controlling their magnetoelectric effects at low temperature. The $RMnO_3$ with larger ionic radius (R = La, Pr, Nd,… and Dy) compounds crystallise in the orthorhombic structure with a space group $Pbnm$, whereas the compounds with smaller ionic radius (R = Dy, Ho, Er and Y) can be obtained either in the orthorhombic or the hexagonal structure with a space group $P6_3cm$[6,7]. In the orthorhombic compounds the Mn ion has the $t_{2g}^3 e_g^1$ electronic configuration. The e_g^1 orbital degeneracy is lifted by the Jahn-Teller distortion[5,8]. These compounds exhibit an orbital ordering at high temperature $T_{OO} \sim 780 - 1500 K$[9–11]. Below T_{OO}, the orbital degree of freedom is spontaneously frozen by the real-space C–type ordering of the e_g orbitals accompanied by the development of a static Jahn-Teller lattice distortion of the MnO_6 octahedra[3,4]. Many previous works have suggested a strong coupling between the spin and the orbital degrees of freedom in the $RMnO_3$ systems[3,8,12–14]. Murakami et al.[8] have reported an experimental evidence of the orbital ordering in $LaMnO_3$ by measuring the (3,0,0) reflection intensity of resonant x-ray scattering[8]. They have found that its integrated intensity, which is related to the order parameter of the orbital ordering, becomes constant below the magnetic ordering temperature $T_N \approx 140 K$ and decreases above it, which suggests that the spin and the orbital orders are intercoupled. The orbital ordering temperature in $RMnO_3$ is significantly enhanced by increasing the $GdFeO_3$-type lattice distortion with decreasing the ionic radius of R (r_R)[3,11]. These lattice distortions increase the orbital ordering frustration and provoke a change of the lattice parameters as shown by x-ray and neutron diffraction measurements[15,16] with a sharp fall in the ordering temperature of the Mn spins[3]. For example, $PrMnO_3$ ($NdMnO_3$) exhibits an A-type antiferromagnetic magnetic structure at $T_N \approx 100 K$ ($T_N \approx 80 K$) in which the spins are aligned ferromagnetically in the basal plane (xz) and antiferromagnetically along the perpendicular direction (y)[17,18]. In more distorted compounds (R = Dy, Tb and Gd) the spin structure becomes sinusoidally modulated in the ab–plane below 39–43 K and spirally modulated below 18-17 K[19]. This last transition coincides with the appearance of a spontaneous electric polarization P_S parallel to the c–axis[1,20]. In these spin-spiral systems the magnetic field is able to flip their electric polarization from c to a–axis.

[1]Université de Sherbrooke, Regroupement Québécois sur les Matériaux de Pointe et Institut Quantique, Département de Physique, Sherbrooke, J1K 2R1, Canada. [2]Prokhorov General Physics Institute of the Russian Academy of Sciences, 38 Vavilov St., Moscow, 119991, Russia. [3]Moscow Power Engineering Institute, 14 Krasnokazarmennaya St., Moscow, 105835, Russia. Correspondence and requests for materials should be addressed to S.M. (email: saber.mansouri@usherbrooke.ca)
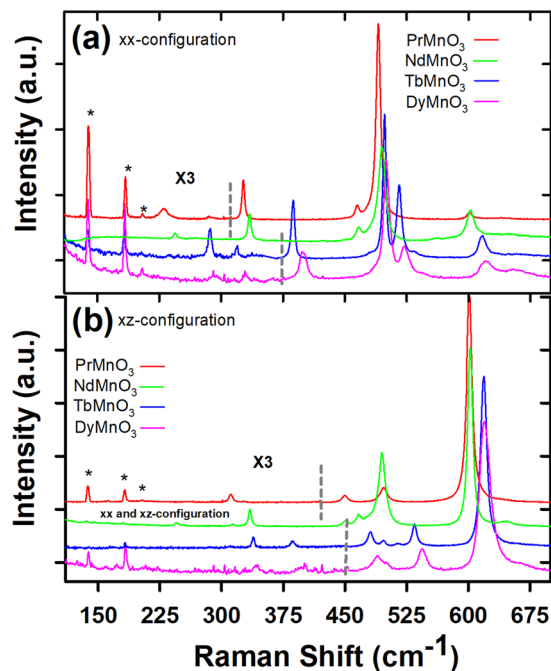
Figure 1. The polarized Raman spectra of $PrMnO_3$, $NdMnO_3$, $TbMnO_3$ and $DyMnO_3$ in the xx (**a**) and xz (**b**) configurations at $T = 5\ K$. (★) indicates plasma lines.

Raman scattering spectroscopy is a powerful tool to investigate the driving force of the interplay of charge, spin, orbital and lattice degrees of freedom[21–25]. The Raman spectra of $RMnO_3$ orthorhombic compounds have been previous studied[21,22,26]. In particular, they have explained the frequency softening of the 490 cm^{-1} and 600 cm^{-1} modes below T_N in terms of spin-phonon coupling caused by the phonon modulation of the superexchange integral[21,22,26]. Recently, Xu *et al.*[27] have attributed the softening behavior of the two excitations at 490 cm^{-1} and 610 cm^{-1} of $LaMnO_3$ to an orbital-spin-phonon (OSP) coupling rather than limited to a spin-phonon coupling only. The verification of the suggested theoretical models requires more studies of the effects of magnetic and orbital orderings on the phonon frequencies in the $RMnO_3$ compounds.

In this paper, we investigate the Raman-active phonons in $PrMnO_3$, $NdMnO_3$, $TbMnO_3$ and $DyMnO_3$ compounds as a function of temperature and magnetic field. The objectives are (i) to study and compare the Raman response of the non-multiferroic systems $PrMnO_3$ and $NdMnO_3$ to those of the multiferroic compounds $TbMnO_3$ and $DyMnO_3$, (ii) to study the effect of a magnetic field on the Raman-active phonons in the representative compounds $PrMnO_3$ and $TbMnO_3$ at low temperature.

Results and Discussion

Based on group-theory, the orthorhombic $RMnO_3$ (space group $Pbnm$) has twenty-four Raman-active modes $(7A_g + 7B_{1g} + 5B_{2g} + 5B_{3g})$[28]. The $RMnO_3$ unit cell contains two MnO_6 octahedra along the y–direction with two apical $O2$ and four equatorial $O1$ oxygen ions at the summits. The $Mn − O2$ bond is along the y–axis while the $Mn − O1$ bonds are in the xz plane (ab–plane).

Figure 1 shows the polarized Raman spectra of $RMnO_3$ ($R = Pr$, Nd, Tb and Dy) in the xx (aa) and xz (ab) configurations at 5 K. The typical phonons associated with the orthorhombic $RMnO_3$ manganites are observed[21,22]. For both configurations, six A_g and six B_{1g} Raman-active phonons are detected. The selection rules are well respected and the phonon linewidths are close to 3–7 cm^{-1} attesting the high crystalline quality of the samples. With decreasing temperature, no additional modes appear indicating a structural phase stability of the $RMnO_3$ compounds. The frequencies of the A_g and B_{1g} Raman active phonons of $PrMnO_3$, $NdMnO_3$, $TbMnO_3$ and $DyMnO_3$ are reported in Table 1. Their vibrational characters are assigned in agreement with previous Raman measurements[29]. With decreasing the ionic radius of R ($r_{Pr} > r_{Nd} > r_{Tb} > r_{Dy}$) most phonon frequencies shift towards higher values. Simultaneously, there is a transfer of intensity between the two high-frequency A_g phonons close to 500 cm^{-1} due to lattice distortions induced by the ionic radius size that mixes the symmetry characters of some phonon excitations[21]. Here we focus on the microscopic mechanisms and the theoretical models required to explain the phonon frequency shifts and how they differ in the multiferroic $TbMnO_3$ and $DyMnO_3$ compounds as compared to the non-multiferroic compounds $PrMnO_3$ and $NdMnO_3$.

Figures 2 and 3 respectively show the temperature dependences of the A_g and B_{1g} phonon frequencies for $PrMnO_3$ (a), $NdMnO_3$ (b) $TbMnO_3$ (c) and $DyMnO_3$ (d). Between 300 K and $T^\star$, the temperature evolutions of the different $RMnO_3$ phonon frequencies are very similar: they harden with decreasing temperature. This frequency hardening is due to the anharmonic effect (dashed line) which can be simulated by the following formula: $\omega(T) = \omega_0 - C\left(1 + \frac{2}{e^x - 1}\right)$, where $x = \frac{\hbar\omega_0}{2K_BT}$, ω_0 and C are adjustable parameters. For $PrMnO_3$ ($NdMnO_3$), the frequencies of the most detected modes soften significantly below $T_N \sim 100\ K$ ($T_N \sim 80\ K$). Remarkably, the fre-

Modes	Atomic displacements[21,22,28]	$PrMnO_3$	$NdMnO_3$	$TbMnO_3$	$DyMnO_3$
A_g	Ag				
(6)	R and $O2$ displacements	147	146	146	143
(2)	in-phase MnO_6 y rotation	228	245	283	288
(7)	$O1(x)$	282	289	317	325
(4)	out of phase MnO_6 x rotations	325	334	385	392
(1)	$O2$ antistretching	463	467	495	494
(3)	$MnO6$ bending	490	494	513	516
B_{1g}	$B1g$				
(6)	R, $O2$ and $O1$ displacements	160	161	164	169
(4)	R and $O2$ displacements	208	210	310	312
(7)	$O1(z)$	309	313	338	338
(3)	out-of-phase $MnO6$ bending	448	450	480	481
(2)	in-phase $O2$ scissorslike	496	502	534	536
(1)	in plane $O2$ stretching	600	602	615	612

Table 1. Frequencies (cm^{-1}) of the Raman-active modes in $PrMnO_3$, $NdMnO_3$, $TbMnO_3$ and $DyMnO_3$ at 5 K.

quencies of $A_g(2)$ at 228 cm^{-1} (245 cm^{-1}), $A_g(3)$ at 490 cm^{-1} (494 cm^{-1}) and $B_{1g}(1)$ at 600 cm^{-1} (602 cm^{-1}) phonons soften by 1.3, 0.5, and 1.0 % (0.7, 0.4 and 0.8 %) respectively below T^N. For $TbMnO_3$, the frequencies of the phonons $A_g(3)$ at 513 cm^{-1}, $B_{1g}(2)$ at 534 cm^{-1} and $B_{1g}(1)$ at 615 cm^{-1} deviate from the regular anharmonic behavior and soften unexpectedly below 130 K. These frequency softenings are slightly pronounced below T_N and much weaker as compared to their corresponding in $PrMnO_3$ and $NdMnO_3$. For example, the frequency softening of the $B_{1g}(1)$ mode is 2 cm^{-1} for $TbMnO_3$ while it is 6 cm^{-1} for $PrMnO_3$. Also, frequencies of the $A_g(4)$ mode and $A_g(7)$ mode show a weak energy softening about 0.6 cm^{-1} below $T_N \sim 40 K$, whereas those of $A_g(1)$, $A_g(2)$, $B_{1g}(3)$ and $B_{1g}(7)$ reproduce an anharmonic behavior. For $DyMnO_3$, the temperature behaviors of the phonon frequencies are similar to those of $TbMnO_3$. Interestingly, the unexpected frequency softenings of the Jahn-Teller phonons ($A_g(3)$ et $B_{1g}(1)$) start well above T_N and are slightly enhanced below T_N.

Analysis of temperature effects. The frequency softening of Raman phonons below T_N in the A–type $RMnO_3$ compounds was previously associated to a spin-phonon coupling[22,26]. Considering the nearest neighbours of the Mn^{3+} ions, Granado *et al.* have shown that the Raman frequency shift is proportional to the square of the Mn^{3+} ferromagnetic sublattice magnetization, $[M(T)]^2$ as defined in eq. (1).

$$(\Delta\omega_\alpha)_{s-ph} \approx -\frac{2}{\mu_\alpha \omega_0}\left(\frac{\partial^2 J_{xz}}{\partial u_{O1}^2} - \frac{1}{2}\frac{\partial^2 J_y}{\partial u_{O2}^2}\right)\left[\frac{M(T)}{4\mu_B}\right]^2 \tag{1}$$

where J_{xz} and J_y are the exchange constants in the equatorial plane and along the apical axis respectively and u_k is the displacement vector from the equilibrium positions of the kth O^{2-} ion. Xu *et al.*[27] have revised the spin-phonon coupling model and have developed a theoretical model that takes into account the contribution of the orbital ordering. The total frequency shift $\Delta\omega_{OSP}(T)$ is written as a function of the effective force constant of the spin-phonon coupling (first term) and the effective force constant of orbital-spin-phonon (second term).

$$\Delta\omega_{OSP}(T) \approx -\frac{1}{2\mu_\alpha \omega_0}\sum_{i,j}\left(\frac{\partial^2 J_1}{\partial u^2}S_i S_j + 4\frac{\partial^2 J_3}{\partial u^2}S_i S_j \tau_i \tau_j\right) \tag{2}$$

where $\tau_i \tau_j$ are the orbital correlation operators and $S_i S_j$ are the spin correlation functions for the i and j Mn^{3+} ions. Using the multivariable Taylor expansion $\sum_{i,j}(S_i S_j \tau_i \tau_j) \approx \sum_{i,j}(\langle S_i S_j\rangle\langle\tau_i\tau_j\rangle + \langle S_i S_j\rangle\delta\tau + \langle\tau_i\tau_j\rangle\delta S)$, where $\delta\tau \equiv \tau_i\tau_j - \langle\tau_i\tau_j\rangle|_{S_i S_j = \langle S_i S_j\rangle}$ and $\delta S \equiv S_i S_j - \langle S_i S_j\rangle|_{\tau_i\tau_j = \langle\tau_i\tau_j\rangle}$, one can establish the expression of the frequency softening of some Raman active modes[27]. The frequency shift $\Delta\omega(T)$ of the in-phase stretching mode at $\sim 600 cm^{-1}$ becomes

$$\Delta\omega_N^{B_{1g}(1)}(T)(-\omega_0)\left(\frac{m}{2}\right) \approx \left[\frac{\partial^2 J_1^{xz}}{\partial u_{O1}^2} + 4\frac{\partial^2 J_3^{xz}}{\partial u_{O1}^2}\left(\langle\tau_i\tau_j\rangle_{xz} + \delta S_{xz}\right)\right]\left[\frac{M(T)}{4\mu_B}\right]^2$$
$$+4\frac{\partial^2 J_3^{xz}}{\partial u_{O1}^2}\langle\tau_i\tau_j\rangle_{xz}\delta S_{xz} \tag{3}$$

and the $\Delta\omega(T)$ of the out-of-phase bending mode at $\sim 490 cm^{-1}$:
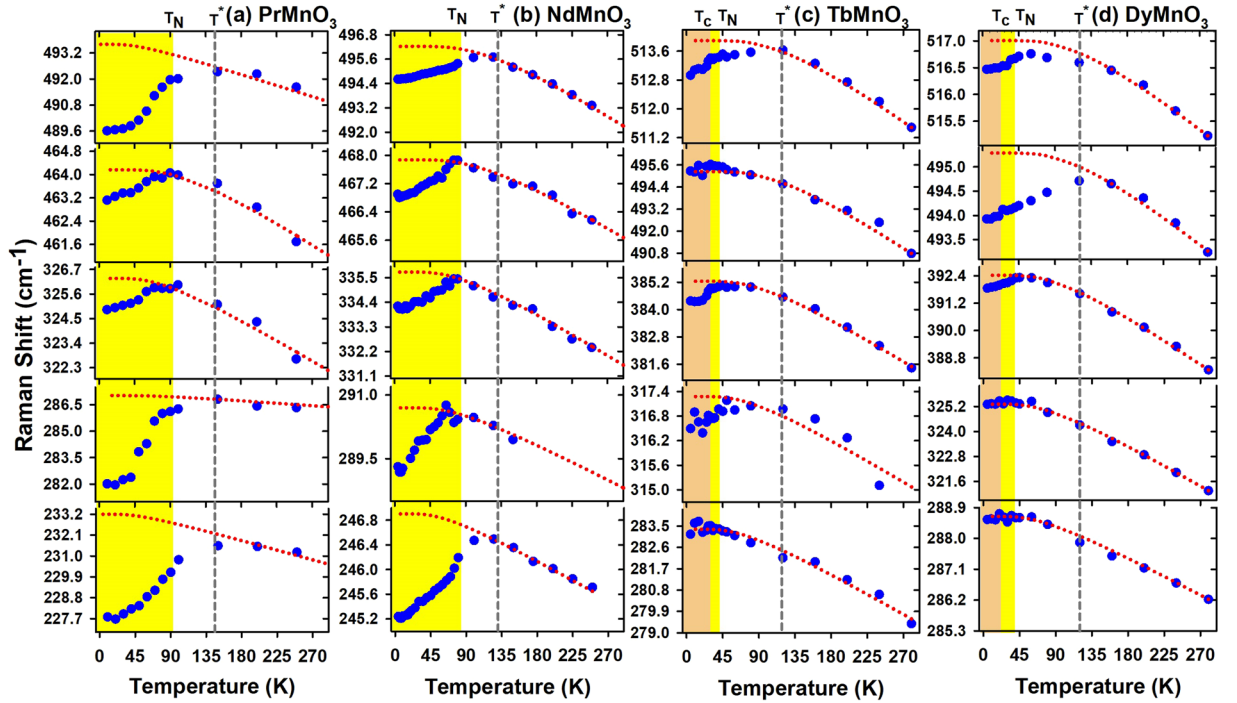
Figure 2. Temperature dependence of the A_g phonon frequencies of $PrMnO_3$, $NdMnO_3$, $TbMnO_3$ and $DyMnO_3$. Dotted lines correspond to the anharmonic behaviour.
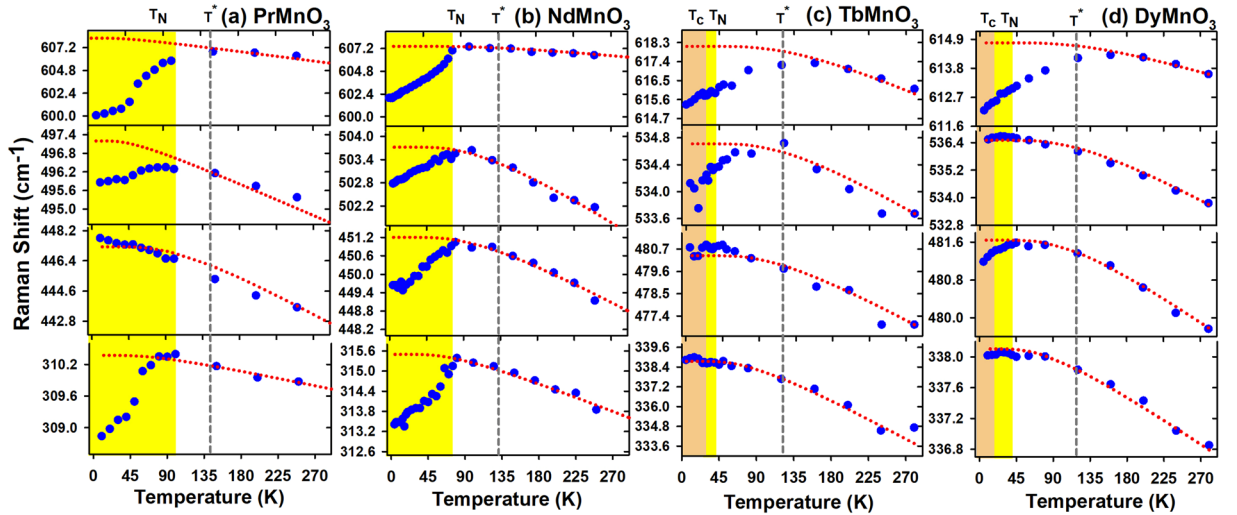

Figure 3. Temperature dependence of the B_{1g} phonon frequencies of $PrMnO_3$, $NdMnO_3$, $TbMnO_3$ and $DyMnO_3$. Dotted lines correspond to the anharmonic behaviour.

$$\Delta\omega_N^{A_g(3)}(T)(-\omega_0)\left(\frac{m}{2}\right) \approx \gamma\left[\frac{\partial^2 J_1^{xz}}{\partial u_{O1}^2} - \frac{1}{2}\frac{\partial^2 J_1^{y}}{\partial u_{O2}^2} + 4\left(\frac{\partial^2 J_3^{xz}}{\partial u_{O1}^2} + \frac{1}{2}\frac{\partial^2 J_3^{y}}{\partial u_{O2}^2}\right)\left(\langle\tau_i\tau_j\rangle_{xz} + \delta S_{xz}\right)\right]$$

$$\left(\frac{M(T)}{4\mu_B}\right)^2 + 4\gamma\left(\frac{\partial^2 J_3^{xz}}{\partial u_{O1}^2} + \frac{1}{2}\frac{\partial^2 J_3^{y}}{\partial u_{O2}^2}\right)\langle\tau_i\tau_j\rangle_{xz}\delta S_{xz}$$

(4)

The common form of these last equations is a linear function $Y = SX + B$ where S is the slope and X is the square of the sublattice magnetization. The intercept B, which is related to the effective force constant of orbital-spin-phonon coupling k_{OSP}, is nonzero only if the interaction exists. This model is successfully used to
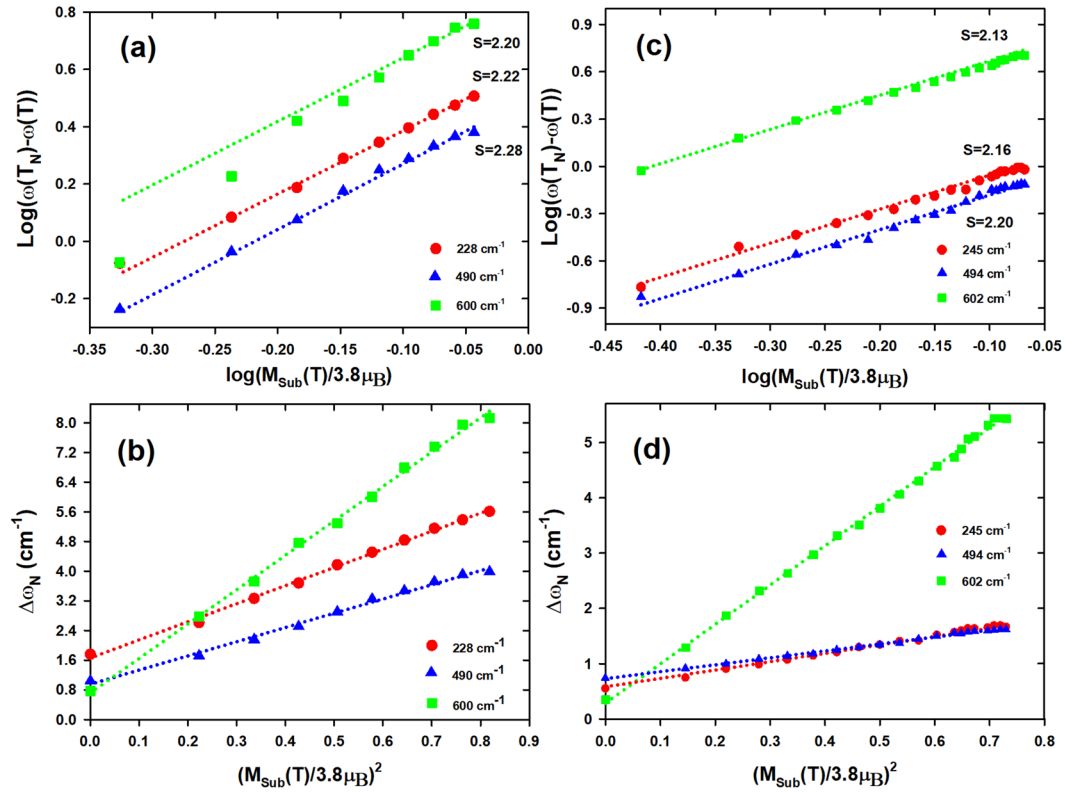
Figure 4. (**a**) A logarithmic plot of the mode frequency softening $\{\omega(T_N) - \omega(T)\}$ with respect to the sublattice magnetization for temperatures between 5 K and 100 K in $PrMnO_3$. (**b**) $\Delta(\omega)$ as a function of $\left(\frac{M_{sub}(T)}{3.8\mu_B}\right)^2$ of the 228 cm^{-1}, 490 cm^{-1} and 600 cm^{-1} modes in $PrMnO_3$. (**c**) and (**d**) represent their corresponding variations in $NdMnO_3$. The variation of $\left(\frac{M_{sub}(T)}{3.8\mu_B}\right)^2$ is taken from Refs[15,22,31].

explain the frequency softening of $LaMnO_3$ phonons[27]. However, detailed studies and more concrete experimental evidences are needed to confirm that the OSP coupling clearly exists, below T_N in the A–type $RMnO_3$ compounds. To assess the validity of the OSP coupling in the case of $PrMnO_3$ (and $NdMnO_3$), we have examined the frequency softening behavior, not only of the high frequency modes at 490 cm^{-1} (494 cm^{-1}) and 600 cm^{-1} (602 cm^{-1}), but also of the low frequency mode at 228 cm^{-1} (245 cm^{-1}) since it corresponds to a rotational Raman-active mode sensitive to the orbital ordering fluctuations as observed in $KCuF_3$[30]. The $\Delta\omega(T)$ of this in-phase MnO_6 y rotation mode can be written as:

$$\Delta\omega_N^{A_g(2)}(T)(-\omega_0)\left(\frac{m}{2}\right) \approx \left[\frac{\partial^2 J_1^{xz}}{\partial u_{RotO1}^2} + 4\frac{\partial^2 J_3^{xz}}{\partial u_{RotO1}^2}\left(\langle\tau_i\tau_j\rangle_{xz} + \delta S_{xz}\right)\right]\left(\frac{M(T)}{4\mu_B}\right)^2$$

$$+ 4\frac{\partial^2 J_3^{xz}}{\partial u_{RotO1}^2}\langle\tau_i\tau_j\rangle_{xz}\delta S_{xz}$$

$$(5)$$

where u_{Rotk} is the displacement vector of the kth O^{2-} ion relative to the rotational mode. According to Granado model (eq. 1), the variation of $\log(\omega(T_N) - \omega(T))$ versus $\log\left(\frac{M_{sub}(T)}{3.8\mu_B}\right)$ should yield a linear line with a slope of $+2$ if the spin-phonon coupling is solely responsible for the frequency softening below T_N. Figure 4(a) (Fig. 4(c)) shows a logarithmic plot of the frequency softening $\{\omega(T_N) - \omega(T)\}$ in $PrMnO_3$ ($NdMnO_3$) for the 600 cm^{-1} (602 cm^{-1}), 490 cm^{-1} (494 cm^{-1}) and 228 cm^{-1} (245 cm^{-1}) modes with respect to the sublattice magnetization $\log\left(\frac{M_{sub}(T)}{3.8\mu_B}\right)$ at temperatures between 5 K and $T_N \sim 100 K$ ($T_N \sim 80 K$). The estimated slope S is significantly different from the prediction value of $+2$. The slope S for a linear fit (dashed line) is around 2.22 (2.16), 2.28 (2.20) and 2.20 (2.13) for the 228 cm^{-1} (245 cm^{-1}), 490 cm^{-1} (494 cm^{-1}) and 600 cm^{-1} (602 cm^{-1}) modes respectively. This suggests that the spin-phonon coupling alone does not adequately explain the observed frequency softening below T_N in $PrMnO_3$ and $NdMnO_3$.

Figure 4(b) shows a good linear correlation between $\Delta\omega(T)$ and $X = \left(\frac{M_{sub}(T)}{3.8\mu_B}\right)^2$ which is in agreement with the linear function of equations 3, 4 and 5. The extrapolation of the linear function at $X = 0$ gives the intercept B:

Compounds/modes	kSP (dynes/cm)			kOSP (dynes/cm)			kOSP/kSP (%)		
Modes	$A_g(2)$	$A_g(3)$	$B1g(1)$	$A_g(2)$	$A_g(3)$	$B1g(1)$	$A_g(2)$	$A_g(3)$	$B1g(1)$
$LaMnO_3$[27]	—	1000	—	—	70	—	—	7.0	—
$PrMnO_3$	651	865	2622	54	66	61	8.2	7.6	2.3
$NdMnO_3$	193	655	2413	20	51	25	10.3	7.7	1.0

Table 2. The effective force constants k_{SP} (spin-phonon coupling) and k_{OSP} (orbital-spin-phonon coupling) of the $A_g(2)$, $A_g(3)$ and $B_{1g}(1)$ Raman-active modes in $LaMnO_3$[27], $PrMnO_3$ and $NdMnO_3$.
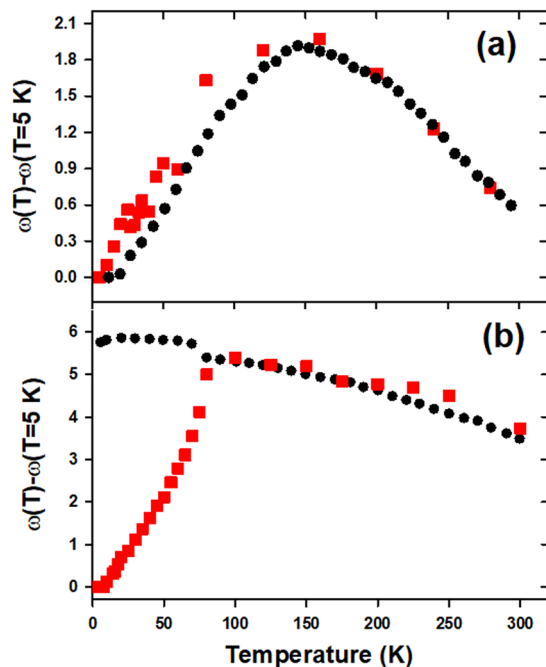

Figure 5. (**a**) The filled red squares show the temperature dependence of the 615 cm^{-1} mode in $TbMnO_3$. The filled black circles show the variation of $-\gamma\omega_0\Delta A/A_0$ as a function of temperature where $A = a \times b$[16]. In (**b**) their corresponding variations in $NdMnO_3$.

1.65, 0.94 and 0.71 for the 228 cm^{-1}, 490 cm^{-1} and 600 cm^{-1} modes respectively. These behaviors are also observed in $NdMnO_3$ with B values: 0.58, 0.73 and 0.29 for the 245 cm^{-1}, 494 cm^{-1} and 602 cm^{-1} modes respectively (Fig. 4(d). These finite positive values indicate that the spin and the orbital orders are also coupled in $PrMnO_3$ and $NdMnO_3$. In addition, the nonzero value of B at T_N implies that this coupling does not vanish completely above T_N but remains nonzero for a finite temperature range due to the magnetic correlations in the paramagnetic phase. The term B is interpreted as the effective force constant of the OSP coupling k_{OSP}. The effective force constants k_{SP} (of spin-phonon coupling) and k_{OSP} (of orbital-spin-phonon coupling) are reported in Table 2. For the three modes, the k_{SP} and the k_{OSP} decrease with the ionic radius of the rare-earth. For all compounds, the k_{OSP} of the $A_g(3)$ ($\sim$490 cm^{-1}) mode is slightly stronger than those of the $A_g(2)$ and $B_{1g}(1)$ modes. This indicates that the $A_g(3)$ mode, intimately related to the Jahn-Teller distortions, is more sensitive to the spin-orbital coupling. The k_{OSP} of the $A_g(3)$ decreases with r_R (of La, Pr and Nd) while the ratio k_{OSP}/k_{SP} is almost constant. These facts underline the important role of the ionic-radius size and the apical O2 vibration in the phonon modulation of the spin-orbital interaction in the $RMnO_3$ A–type compounds.

As mentioned above, the frequency softenings of phonons in $TbMnO_3$ and $DyMnO_3$ are much weaker than those in $PrMnO_3$ and $NdMnO_3$. The origin of their frequency softening remains unclear: it has been qualitatively assigned to a spin-phonon coupling[32] or to an expansion in the $Mn - O$ bond lengths[22]. However, there are no concrete experimental proofs to determine their true origin. The phonon frequency shifts induced by the change of the ionic binding energies due to the lattice expansion/contraction, is usually approximated by the Grüneisen law $\Delta\omega_\alpha(T)/\omega_0 = -\gamma_\alpha(\Delta V/V_0)$ where γ_α is the Grüneisen parameter for the normal mode α. This later approximation is applicable for isotopically expanded lattices. One should also consider the possibility of phonon frequency shifts due to lattice anomalies, even in the absence of a lattice unit cell volume change. Indeed, for some phonons the displacement of the involved atoms is either unidimensional or restricted in a plane. Blasco et al.[16] have observed an expansion in $TbMnO_3$ a–lattice parameter below 130 K and no significant changes are observed for the b and c parameters.

Figure 5 shows the temperature dependence of the frequency of $B_{1g}(1)$ mode (red squares) in $TbMnO_3$ (a) and $NdMnO_3$ (b). The black dots indicate the variation of $-\gamma\omega_0\Delta A/A_0$ as a function of temperature where $A = a \times b$
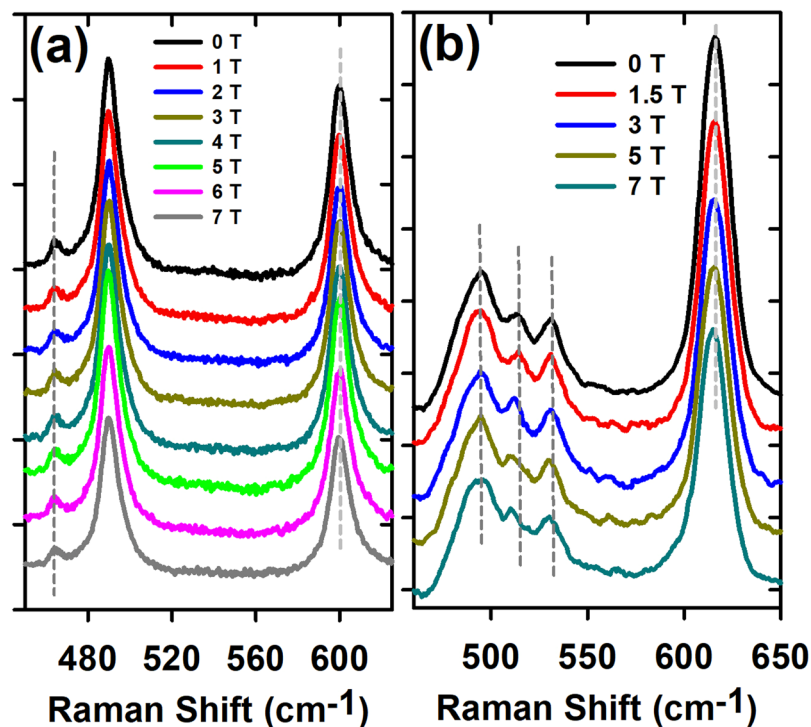
Figure 6. Unpolarised Raman spectra of $PrMnO_3$ (**a**) and $TbMnO_3$ (**b**) as a function of magnetic field (up to 7 T) applied along the c−axis.

and γ is the Grüneisen parameter. The frequency softenings of the $B_{1g}(1)$ mode are in agreement with the thermal expansion in the ab−plane with a Grüneisen parameter of ~ 0.0416 in the case of $TbMnO_3$ whereas it is clearly not the case of $NdMnO_3$ below $T \sim 80\,K$. This confirms that in the case of $TbMnO_3$ the frequency shift of the $B_{1g}(1)$ mode is mainly due to an expansion in the $Mn - O$ distances related to discrete orbital rearrangements close to the magnetic order transition, a phenomenon not discussed before, in this much-distorted compounds $RMnO_3$ ($R = Tb$ and Dy). Indeed, the negative thermal expansion, recently observed in some magnetic materials ($Ca_2Ru_{1-x}M_xO_4$ where $M = Mn$ and Fe) at low temperatures, is attributed to a strong coupling between orbital and magnetic orders[33,34]. In addition, the frustrated magnetic order in $TbMnO_3$ is usually attributed to its frustrated orbital ordering as compared to $TbMnO_3$[3].

Analysis of magnetic-field effects.

In order to further investigate the spin-lattice coupling in a frustrated multiferroic system $TbMnO_3$ againt a non-multiferroic compound $PrMnO_3$, we also study the evolutions of Raman active phonon frequencies of both compounds under an applied magnetic field at 4.2 K, below $T_N^{R=Pr,Tb}$.

Figure 6 shows the magnetic field dependence of the unpolarized macro-Raman spectra of $PrMnO_3$ (a) and $TbMnO_3$ (b) up to 7 Tesla. The applied magnetic field is quasi-parallel to the c−axis. While some of $TbMnO_3$ phonon frequencies are shifted as a function of magnetic field, those of $PrMnO_3$ remain unaffected. Similarly to $TbMn_2O_5$[35], these magnetic-field induced frequency shifts reflect the frustration of the spin configuration in $TbMnO_3$ and its sensitivity to the presence of a magnetic field. The most affected phonons in $TbMnO_3$, by the magnetic field, are the Jahn-Teller modes at 615 cm^{-1} ($B_{1g}(1)$) and 513 cm^{-1} ($A_g(3)$). Their frequencies soften by $\sim 1\,cm^{-1}$ and $\sim 2\,cm^{-1}$ at 7 Tesla respectively. These phonons involve mainly the $O1$ oxygen vibrations in the xz−plane and the $Mn - O$ distances suggesting a magnetic-field modulation of the $Mn - O - Mn$ bond lengths. These findings are in agreement with previous results indicating that a magnetic field induces a magnetoelastic coupling in $TbMnO_3$[36,37]. Also, in our study of the Tb^{3+} crystal-field excitations in $TbMnO_3$ single crystals, we have found that some excitations are significantly shifted under an applied magnetic field along the c−axis at 4.2 K[38]. This observation is in favor of oxygen displacements under magnetic-field in agreement with a prominent role of the oxygen ions in the multiferroicity of $TbMnO_3$ and $DyMnO_3$ as recently reported by Huang et al.[39]. Hence the ferroelectricity is related to local oxygen arrangements following the increase of the $Mn - O1$ bond length as induced by Dzyaloshinskii-Moriya interaction rather than a pure electronic mechanism as suggested by Kastura et al.[40,41].

Conclusion

In this comparative Raman study of the $PrMnO_3$, $NdMnO_3$, $TbMnO_3$ and $DyMnO_3$ single crystals, the phonon frequency shifts in $PrMnO_3$ and $NdMnO_3$ observed below T_N, are explained by an orbital-spin-phonon coupling whereas those in $TbMnO_3$ and $DyMnO_3$, observed below 130 K, are attributed to an expansion of the $Mn - O$ distances. In our $PrMnO_3$ and $TbMnO_3$ magneto-Raman measurements, it is shown that some $TbMnO_3$ phonons are shifted as a function of magnetic field, while those of $PrMnO_3$ remain unaffected. The magnetic-field dependence

of the $TbMnO_3$ phonon frequencies is associated to a magnetic modulation of the $O1$ oxygen displacements and suggests that $Mn - O1$ bond polarization may play a significant role in the magnetoelectric properties of $TbMnO_3$.

Methods

$RMnO_3$ ($R = Pr$, Nd, Dy and Tb) single-crystals were grown by the floating zone method as described in reference[42]. The Raman spectra were recorded at temperatures between 300 K and 5 K and were obtained in the backscattering configuration using a $He - Ne$ laser (632.8 nm) and a Labram-800 micro-Raman spectrometer equipped with a $X - 50$ objective microscope (focus diameter around ~3 μm), an appropriate notch filter and a nitrogen-cooled CCD detector. The studied single crystals were mounted in a continuous flow temperature regulated liquid helium Janis cryostat. We have also measured the Raman active excitations under applied magnetic field up to 7 Tesla. The Raman measurements under magnetic field were obtained with an Ar^+ incident laser (514.5 nm) and with a magnetic field parallel to the c–axis.

Data Availability.   Most data generated or analysed during this study are included in this published article. The Raman spectra of $RMnO_3$ ($R = Pr$, Nd, Dy and Tb) compounds at different temperatures are available from the corresponding author on reasonable request.

References

1. Kimura, T. *et al*. Magnetic control of ferroelectric polarization. *nature* **426**, 55–58 (2003).
2. Balli, M. *et al*. Large rotating magnetocaloric effect in the orthorhombic *dymno₃* single crystal. *Solid State Communications* **239**, 9–13 (2016).
3. Kimura, T. *et al*. Distorted perovskite with e_g^1 configuration as a frustrated spin system. *Physical Review B* **68**, 060403 (2003).
4. KI, K. & Khomskii, D. The jahn-teller effect and magnetism: transition metal compounds. *Sov. Phys. Usp* **25**, 231 (1982).
5. Khomskii, D. & Sawatzky, G. Interplay between spin, charge and orbital degrees of freedom in magnetic oxides. *Solid state communications* **102**, 87–99 (1997).
6. Gilleo, M. Crystallographic studies of perovskite-like compounds. iii. *la(m_x, mn_{1-x})o₃* with m = co, fe and cr. *Acta Crystallographica* **10**, 161–166 (1957).
7. Yakel, H., Koehler, W., Bertaut, E. & Forrat, E. On the crystal structure of the manganese (iii) trioxides of the heavy lanthanides and yttrium. *Acta Crystallographica* **16**, 957–962 (1963).
8. Murakami, Y. *et al*. Resonant x-ray scattering from orbital ordering in *lamno₃*. *Physical review letters* **81**, 582 (1998).
9. Sánchez, D., Alonso, J. & Martnez-Lope, M. Neutron-diffraction study of the jahn–teller transition in *prmno₃*. *Journal of the Chemical Society, Dalton Transactions* 4422–4425 (2002).
10. Zhou, J.-S. & Goodenough, J. Unusual evolution of the magnetic interactions versus structural distortions in *rmno₃* perovskites. *Physical review letters* **96**, 247202 (2006).
11. Seman, T. *et al*. Effects of rare-earth ion size on the stability of the coherent jahn-teller distortions in undoped perovskite manganites. *Physical Review B* **86**, 184106 (2012).
12. Brzezicki, W., Dziarmaga, J. & Oleś, A. M. Exotic spin orders driven by orbital fluctuations in the kugel-khomskii model. *Physical Review B* **87**, 064407 (2013).
13. Okamoto, S., Ishihara, S. & Maekawa, S. Orbital ordering in *lamno₃*: Electron-electron and electron-lattice interactions. *Physical Review B* **65**, 144403 (2002).
14. Mondal, P., Bhattacharya, D., Choudhury, P. & Mandal, P. Dielectric anomaly at t_N in *lamno₃* as a signature of coupling between spin and orbital degrees of freedom. *Physical Review B* **76**, 172403 (2007).
15. Chatterji, T., Ouladdiaf, B. & Bhattacharya, D. Neutron diffraction investigation of the magnetic structure and magnetoelastic effects in *ndmno₃*. *J. Physics: Condens. Matter* **21**, 306001 (2009).
16. Blasco, J. *et al*. Structural and magnetic study of *tb_{1-x}ca_xmno₃* perovskites. *Physical Review B* **62**, 5609 (2000).
17. Dyakonov, V. *et al*. Structural and magnetic properties of *la_{1-x}pr_xmno_{3+δ}* (0 ≤ x ≤1.0). *Physical Review B* **74**, 024418 (2006).
18. Hemberger, J. *et al*. Magnetic properties and specific heat of *rmno₃* (r = pr, nd). *Physical Review B* **69**, 064418 (2004).
19. Kenzelmann, M. *et al*. Magnetic inversion symmetry breaking and ferroelectricity in *tbmno₃*. *Physical Review Letters* **95**, 087206 (2005).
20. Kimura, T. *et al*. Magnetoelectric phase diagrams of orthorhombic *rmno₃* (r = gd, tb, and dy). *Physical Review B* **71**, 224425 (2005).
21. Iliev, M. *et al*. Distortion-dependent raman spectra and mode mixing in *rmno₃* perovskites (r = la, pr, nd, sm, eu, gd, tb, dy, ho, y). *Physical Review B* **73**, 064302 (2006).
22. Laverdiere, J. *et al*. Spin-phonon coupling in orthorhombic *rmno₃* (r = pr, nd, sm, eu, gd, tb, dy, ho, y): A raman study. *Physical Review B* **73**, 214301 (2006).
23. Vermette, J., Jandl, S., Orlita, M. & Gospodinov, M. Role of the apical oxygen in the low-temperature magnetoelectric effect in *rmno₃* (r = ho and lu). *Physical Review B* **85**, 134445 (2012).
24. Mansouri, S. *et al*. Raman and crystal field studies of *tb–o* bonds in *tbmn₂o₅*. *Physical Review B* **94**, 115109 (2016).
25. Elsässer, S. *et al*. Impact of temperature-dependent local and global spin order in *rmno₃* compounds for spin–phonon coupling and electromagnon activity. *New Journal of Physics* **19**, 013005 (2017).
26. Granado, E. *et al*. Magnetic ordering effects in the raman spectra of spectra of *la_{1-x}mn_{1-x}o₃*. *Physical Review B* **60**, 11879 (1999).
27. Xu, J., Park, J. H. & Jang, H. M. Orbital-spin-phonon coupling in jahn-teller-distorted *lamno₃*: Softening of the 490 and 610 cm-1 raman-active modes. *Physical Review B* **75**, 012409 (2007).
28. Iliev, M. *et al*. Raman spectroscopy of orthorhombic perovskitelike *ymno₃* and *lamno₃*. *Physical Review B* **57**, 2872 (1998).
29. Rovillain, P. *et al*. Electromagnon and phonon excitations in multiferroic *tbmno₃*. *Physical Review B* **86**, 014437 (2012).
30. Lee, J. C. *et al*. Two-stage orbital order and dynamical spin frustration in *kcu f₃*. *Nature Physics* **8**, 63–66 (2012).
31. Jirak, Z. *et al*. Neutron diffraction study of *pr_{1-x}mn_xo₃* perovskites. *Journal of Magnetism and Magnetic Materials* **53**, 153–166 (1985).
32. Kumar, P. *et al*. Raman evidence for orbiton-mediated multiphonon scattering in multiferroic *tbmno₃*. *Journal of Physics: Condensed Matter* **22**, 115403 (2010).
33. Qi, T. *et al*. Negative volume thermal expansion via orbital and magnetic orders in *ca₂ru_{1-x}cr_xo₄* (0 < x < 0.13). *Physical review letters* **105**, 177203 (2010).
34. Qi, T. *et al*. Magnetic and orbital orders coupled to negative thermal expansion in mott insulators *ca₂ru_{1-x}m_xo₄* (m = mn and fe). *Physical Review B* **85**, 165143 (2012).
35. Mansouri, S. *et al*. Micro-raman and infrared studies of multiferroic *tbmno₃*. *Journal of Physics: Condensed Matter* **28**, 055901 (2016).
36. Rovillain, P. *et al*. Magnetic field induced dehybridization of the electromagnons in multiferroic *tbmno₃*. *Physical review letters* **107**, 027202 (2011).
37. Aliouane, N. *et al*. Field-induced linear magnetoelastic coupling in multiferroic *tbmno₃*. *Physical Review B* **73**, 020102 (2006).
38. Mansouri *et al*. Study of crystal-field excitations and infrared active phonons in *tbmno₃*. to be published x, xxxx (xxxx).

39. Huang, S.-W. *et al*. Prominent role of oxygen in the multiferroicity of *dymno*₃ and *tbmno*₃: A resonant soft x-ray scattering spectroscopy study. *Physical Review B* **94**, 035145 (2016).
40. Sergienko, I. A. & Dagotto, E. Role of the dzyaloshinskii-moriya interaction in multiferroic perovskites. *Physical Review B* **73**, 094434 (2006).
41. Katsura, H., Nagaosa, N. & Balatsky, A. V. Spin current and magnetoelectric effect in noncollinear magnets. *Physical review letters* **95**, 057205 (2005).
42. Balbashov, A., Karabashev, S., Mukovskiy, Y. M. & Zverkov, S. Growth and giant magnetoresistance effect in *lacamno* and *lasrmno* single crystals. *Journal of crystal growth* **167**, 365–368 (1996).

Acknowledgements

Author Contributions

S.M. and S.J. conceived the study. A.M., V.Y.I., and A.B. prepared the samples. S.M. performed the measurements. S.M. and S.J. analyzed the results. S.M. wrote the manuscript. All authors commented on the manuscript.

Additional Information

Competing Interests: The authors declare that they have no competing interests.

Publisher's note: Springer Nature remains neutral with regard to jurisdictional claims in published maps and institutional affiliations.